Final Technical Report
Date of Report: October 20, 2022

Federal Agency/ Organization Element:	DOE/EERE/ Advanced Manufacturing Office (AMO)
FOA Name and Number:	FY19 Advanced Manufacturing Office Multi-Topic FOA Funding Opportunity Announcement (FOA) Number: DE-FOA-0001980
DOE Award Number:	DE-EE0009108
Project Title:	Innovative Design and Manufacturing of 2.5D Battery with High Energy and Power Density
Project Period:	06:2020 – 08:2022
Recipient Organization:	Regents of the University of California Los Angeles
Recipient Type:	Public/State Controlled Institution of Higher Education
DUNS Number:	092530369
Principal Investigator	Dr. Bruce Dunn bdunn@ucla.edu, 310-825-2938
Business Contact:	**Rachel Tat, Grant Officer** rachel.tat@research.ucla.edu, 310-794-6392
Team Member Organizations:	Regents of the University of California Los Angeles Lawrence Livermore National Laboratory
DOE Technology Manager:	Tina Kaarsberg, tina.kaarsberg@ee.doe.gov: 202-586-8106
DOE Project Manager:	Bill Prymak, bill.prymak@ee.doe.gov: 240-562-1754
DOE Project Monitor:	Eric Peterson, Eric.Peterson@ee.doe.gov: 240-562-1800
DOE Award Administrator:	Laura Gonzalez, laura.gonzalez@ee.doe.gov, 240-562-1310
Submitting Official:	Rachel Tat, Grant Officer, rachel.tat@research.ucla.edu, 310-794-69392

The Submitting Official certifies that the information provided in the Research Performance Progress Report is accurate and complete as of the date shown.

Acknowledgment:

This material is based upon work supported by the U.S. Department of Energy's Office of Energy Efficiency and Renewable Energy (EERE) under the Advanced Manufacturing Office Award Number DE- EE0009108.

Table of Contents

List of Acronyms

UCLA…University of California Los Angeles
LLNL…Lawrence Livermore National Laboratory
LFP…Lithium Iron Phosphate, $LiFePO_4$
DIW…Direct Ink Writing
AM… Additive Manufacturing
LIB…Lithium Ion Battery
3D…Three Dimensional
2D…Two Dimensional
2.5D…Two and a Half Dimensional
$LiClO_4$…Lithium Perchlorate
EC:DMC…Ethylene Carbonate: Dimethyl Carbonate
LiTFSI…Lithium bis(trifluoromethanesulfonyl)imide
BMImTFSI…1-Butyl-3-methylimidazolium bis(tribluoromethylsulfonyl)imide
Dakota… Dakota Lithium
AE…American Elements
XRD…X-Ray Diffraction
PVDF…Polyvinylidene Fluoride
PC…Propylene Carbonate
SEM…Scanning Electron Microscopy
CV…Cyclic Voltammetry
PDMS…Polydimethylsiloxane
GITT… Gravimetric Intermittent Titration Technique
ILE…Ionic Liquid Electrolyte

List of Figures

Figure 15. (a) Outlines the ionogel solvent exchange process to remove the ILE from the silica matrix and exchange in organic electrolyte. (b) Galvanostatic charge/discharge curves comparing an LFP electrode with an ionogel with ionic liquid, a solvent exchanged ionogel, and in organic electrolyte at a rate of C/10.

Figure 16. Optimized fabrication process flow for full 2.5D battery.

Figure 17. (a) Predicted areal capacity of 2, 3 and 5 layer lattices with varying pitch length. The red star is the experimental areal capacity of a 5 layer lattice. (b) Specific capacity and coulombic efficiency of device with a 5 layer lattice.

List of Tables

Executive Summary

The goal of this project is to develop cathode inks, to be used in additive manufacturing (AM), that lead to a low-cost, fast manufacturing processes for a new type of non-planar, 2.5D lithium-ion battery (LIB). 2.5D batteries, comprised of a high-aspect-ratio 3D electrode combined with a 2D planar electrode, can simplify the fabrication process because there is no need for the alignment steps seen in traditional 3D batteries. For the success of the two AM processes identified in this project, development of cathode inks is key component because it allows for both platforms to be evaluated in achieving high performance batteries and ease of manufacturing. The two AM processes explored in this project are direct ink writing (DIW) and templating. Both of these processes have been shown to be successful in depositing materials for traditional LIBs and will be used now for the 3D array electrode configuration as part of the 2.5D battery.

The advantage of the chosen AM methods is that devices can be made with high volume, quickly and with little capital equipment costs. DIW in particular can enable cost reduction of >90% for high-aspect-ratio structures fabricated using other methods such as photolithography or etching. Therefore, the first generation 2.5D battery can be made without considering the limitations of expensive manufacturing for micro-fabrication. Through this program, the main outcomes can be divided into three main goals: (1) the development of cathode inks, (2) printing electrode arrays, and other components of 2.5D batteries, assemble these components into the proposed architecture and (3) testing the battery for its performance.

While DIW for battery manufacturing is still in an R&D phase, early work by Lawrence Livermore National Lab (LLNL) has shown that it has the ability to support larger production at a portion of the traditional manufacturing costs. That feature alongside the low capital equipment cost of DIW printers, shows that utilizing the DIW process can directly help reduce costs of battery manufacturing. An example of a large volume production at LLNL was of silicone cushions. The volume production of cushions has been integrated into weapon systems for national security applications.

Most of the advances in 3D battery technology have occurred in areas related to consumer electronics as this platform was developed initially for microbattery applications because of its small footprint area. Accompanying those advancements was the emergence of many microbattery and solid state battery startup companies for a variety of applications. One of the

largest problems with the development of non-planar batteries for consumer electronics has been the scalable production.

Building off of this, the DOE targets for fast charging batteries are 200Wh/kg at 4C but these are for batteries with liquid electrolytes. The focus of this program focuses on a lab scale 3D battery design with an ionogel electrolyte and thus offers a much safer, solid-state design. This work will serve as the basis to using DIW as a route for the scalable production of a different 3D battery design, that of interdigitated arrays of anodes and cathodes. Through this project, a viable cathode ink of Lithium Iron Phosphate (LFP) was successfully created for printing via DIW. The 3D printed lattice structures were shown to achieve lithium capacities of as high as 90% of the theoretical lithium capacity for LFP. By optimizing the cathode structure, baseline metrics have been identified for scale up and eventual commercialization to achieve the DOE targets stated above.

The early research on 2.5D batteries was carried out as part of the EFRC headed by the University of Maryland (Nanostructures for Electrical Energy Storage or NEES). Thus, the following EERE project leverages the success of this initial research phase and moves it towards fabricating the most critical component of the battery, the electrode array, by a robust and rapid manufacturing technology. The project also leverages LLNL's expertise in 3D printing technology. The application of additive manufacturing in battery fabrication has received relatively limited investigation despite the promise that this methodology holds for manufacturing the next generation of energy storage technology. In this way, the proposed EERE project complements LLNL's additive manufacturing efforts and adds to its experience in battery manufacturing. Moreover, this project provides an opportunity for LLNL to further develop cutting edge cathode inks, a critical component for incorporating additive manufacturing into battery fabrication. The proposed project is expected to advance 2.5D battery technology and provide the basis for fabricating larger prototype devices that offer greater amounts of energy. Thus, the DOE funding enables us to move from a research phase to an intermediate stage where battery performance and operation is reproduced using a more feasible fabrication route. An important outcome from the project is that of evaluating the scale-up of the 2.5D energy storage approach from which the feasibility of prototype development can be determined. Such prototype demonstration should be attractive to industry for further development.

Chapter 1. *Introduction*

LIBs are known for their high energy density but tend to lack the power density required for future electrical vehicles and consumer electronics, especially with regard to fast charging and discharging. A recharging time of < 15 minutes without compromising energy density and providing appropriate driving range and cost targets is of central importance in advancing energy storage technologies for battery electric vehicles. In recent years, there has been significant interest in three-dimensional (3D) batteries where the electrodes have a non-planar configuration. By balancing line dimensions, height, aspect ratio, and pitch (distance between lines), it is possible to increase both energy and power density (area normalized) relative to conventional batteries with planar geometry. Because of the effective use of the "z" direction, 3D batteries have relatively small footprints and thus are being actively investigated for applications where compact designs are beneficial.[1] However, the fabrication of such 3D batteries is nontrivial, and the use of microfabrication techniques is not cost effective. Moreover, defects that are prone to occur during manufacturing diminish the performance of many 3D batteries. In this program we are able to take advantage of AM methods to produce 3D electrode configurations which provide the design basis for the 2.5D battery and lead to improvements in manufacturing and cost.

To overcome the limitations of 3D batteries, 2.5D battery structures have been developed. This design consists of one 3D electrode structure (cathode) and a planar electrode (anode) with the electrolyte filling the remaining volume. This arrangement greatly simplifies the battery fabrication process and thus reduces cost. Although microfabrication methods enabled the 2.5D concept to be demonstrated, these methods will not lead to the high volume, robust manufacturing approaches required for next generation energy storage technologies. For this reason, an important objective for this project is to use AM methods to print 3D cathode architectures. The DIW and templating methods identified in this program offer high volume, high precision, rapid, and repeatable manufacturing processes which need little capital equipment cost. A COMSOL model of the 2.5D geometry showed that the key consideration for this geometry is having a solid electrolyte with high conductivity.[2] With this consideration in mind, this project will involve the use of pseudosolid ionogel electrolytes.[3] These materials make use of sol-gel processing, leading to macroscopically solid materials whose ionic conductivity is comparable to the liquid electrolyte encapsulated within nanoscale pores of the material. It was

subsequently demonstrated a 2.5D battery that operated at energy and power levels which validated the earlier models.[4]

While the microfabrication methods used to fabricate this first generation of 2.5D batteries enable the 2.5D concept to be demonstrated, these methods will not lead to the high volume, robust manufacturing approaches required for next generation energy storage technologies. For this reason, the focus of this project is to use the direct ink writing (DIW) process to print 3D arrays of cathode rods. DIW is a rapid prototyping tool that allows us to generate and test designs and materials systems for use as electrode arrays, thus enabling us to determine the parameter space for battery manufacturing. DIW can also be a high volume, high precision, rapid, and repeatable manufacturing process, which needs little capital equipment cost. DIW can produce intricate structures made of ceramics, metal, polymers, and composites for technologies such as filtration, catalysis, heat exchange, and more. Of relevance to the current project is that DIW has also been demonstrated as a successful method of depositing electrochemical energy storage materials incorporated into Li-ion batteries, although nearly all these studies have been with planar geometries.[5-7]

The primary goal of this project is to develop low-cost, fast manufacturing processes for a new type of non-planar, 2.5D battery via a DIW additive manufacturing process. The DIW process avoids costly manufacturing limitations of current micro-fabrication processes such as photolithography. Thus, a key outcome for this project is the fabrication of 2.5D batteries. Another important goal of the project is to evaluate the DIW process for scale-up and producing larger scale battery platforms. The use of the 3D array electrode to achieve fast charging is attractive for transportation while the solid-state battery designs for the 2.5D battery offer improved safety for virtually all energy storage application areas.

Chapter 2. *Background*

UCLA has been at the center of 3D battery development. A seminal paper in 2004 presented various designs, materials processing and advantages of 3D configurations.[2] Subsequently, a number of these and other 3D battery designs were demonstrated experimentally, including interdigitated 3D anodes and cathodes, trench-like designs, and concentric tubes.[3, 4, 8, 9] The focus of research efforts from the Dunn group have been directed primarily at developing and characterizing high-aspect-ratio electrode materials capable of delivering high areal energy and power densities.[8-11] Recently, in collaboration with groups from Sandia National Laboratory and University of Utah, all-solid-state 3D Li-ion batteries based on $LiCoO_2$ and Si electrode materials and LIPON solid electrolytes have been demonstrated using microfabrication techniques.[12] However, poor power performance was observed in comparison to similarly prepared planar batteries. A simulation of the 3D battery design indicated that a combination of structural inhomogeneities (from fabrication challenges) and low electrolyte conductivity led to a nonuniform current density distribution and, thus, poor electrode material utilization.[12] A follow-up computational study extended the simulation to the 2.5D geometry and showed the importance of having an electrolyte with high ionic conductivity.[13] The Dunn group has recently reported the development of ionogel solid electrolytes which exhibit high ionic conductivity.[14] This electrolyte was incorporated in the 2.5D battery design, leading to the fabrication of a solid-state 2.5D battery. It is important to note that we have full access to the 2.5D battery simulation developed by our colleagues.

LLNL has a well-established history in 3D printed materials. Early work showed that 3D printed materials can exhibit ultra-stiff properties across more than three orders of magnitude in density, for a variety of materials,[15-17] and that printed architectures can control structural flexibility, even for typically stiff materials. Specifically, 3D printing of fractal-like lattices with features ranging from the nanometer to centimeter scale enabled the creation of a nickel-plated metamaterial with a high elasticity not found in any previously built metal foams or lattices. The particular technique developed to fabricate this structure, large area projection micro-stereolithography (LAPμSL), garnered an R&D 100 award in 2015. More recently, LLNL has used 3D printed electrodes to build a MnO_2 -based device with improved ion transport facilitated by the 3D printed structure.[18] In addition, volume additive manufacturing, holographic patterning of light fields in a resin, allows the one-step fabrication of complex parts.[19] This technique

represents a paradigm shift in 3D printing, transitioning from a layer-by-layer approach (i.e. 2D patterns built up into a 3D part) to a truly 3D process. This work demonstrates the possibility of printing extremely complex structures of relevant high surface area electrode materials.[20] In this project, LLNL will continue to demonstrate the impact that 3D printed functional materials can have on energy storage devices and extend our innovations in developing novel feedstocks for 3D printing techniques.

The development of electrode inks containing active material, carbon, and binder has been well established, particularly for planar battery architectures. Typically, the ink viscosity and feature resolution for continuous filament writing are targeted at 10^2 to 10^6 mPa s and 10 μm to 1 mm, respectively, to achieve conformal deposition.[21, 22] However, due to the planar geometry and thin-film nature of the electrodes, energy densities of these devices are limited to ~20 - 40 μAh cm^{-2}. [23, 24] Preliminary work on 3D battery architectures has demonstrated improvements in the areal energy density. For example, an inkjet-printed zinc-silver 3D battery demonstrated 2.4 mAh cm^{-2} on initial cycling, but a capacity loss of 20% occurred after just 7 cycles due to delamination of the pillars from the glass substrate.[25] A lithium titanate (LTO)/lithium iron phosphate (LFP) full cell with interdigitated 3D pillars has also been synthesized with inkjet printing, demonstrating 1.5 mAh cm^{-2}. [26] In addition, an LTO/Li metal half-cell with an aspect ratio of ~1.9 and an areal capacity of 1 mAh cm^{-2} demonstrated 80% capacity retention after 200 cycles at 1C.[27]

Taken together, the above results indicate that the development of inks for electrochemical energy storage is at a very early stage. Moreover, fabrication of high-aspect-ratio battery electrodes (>3:1) via additive manufacturing, a key objective in this project, has been very limited; we are aware of only one report on interdigitated 3D morphologies.[26] In order to print high-aspect-ratio cathode structures using DIW, the ink formulation and rheology need to be precisely controlled. In addition to possessing proper electrical and electrochemical properties, the inks must be mechanically robust and shear thinning, so that they are easily extruded but maintain their shape after printing and drying. Furthermore, they must have an appropriate composition to generate porous cathode materials after drying to allow electrolyte penetration for ionic conductivity. Developing inks that can meet all these requirements is challenging and requires careful materials selection and formulation.

The high-aspect ratio 3D electrode architecture enables us to increase the areal energy density of the battery without sacrificing power density. However, the loading of the electrode cannot be increased without limit, as the ohmic resistance resulting from the height of electrodes will become significant, especially at high current densities. The principal innovation involved in the development of cathode inks is the use of novel additives which improve the electronic conductivity. Carbons are widely used for this purpose but, in fact, there are several possible materials which can be incorporated for the same function.

Inks previously presented by LLNL represent a wide range of pore sizes, particle sizes, densities, electrical and mechanical properties. However, it has not been demonstrated that these inks can be applied to print the 3D electrode arrays originally proposed in this work. The main needs here are to ensure that the conductivity, mechanical robustness, and chemical stability after 3D printing are sufficient for use in the 2.5D battery. With the variety of available inks coupled with LLNL experience, there is a wide parameter space in which we can identify the optimal electrode for the 2.5D battery application. Another need/challenge is to control the pitch and array dimensions through 3D printing techniques.

Three-dimensional batteries were designed with the intent of using the third dimension, height, to increase the amount of electrode material within a given footprint area. These designs were primarily considered for microscale devices with footprint areas on the order $1cm^2$. Moreover, because 3D electrodes were configured to minimize the ionic path length between electrodes, there is the prospect of achieving high energy and power density within the small footprint area. Few 3D batteries have been reported[3, 4, 8, 9] as the fabrication of these electrochemical devices is difficult because of aligning anode and cathode arrays and the need to have a conformal solid electrolyte coating over high aspect ratio rods in the arrays. The 2.5D battery overcomes these limitations. Our work, which is not yet reported in the open literature,[11] recently demonstrated the advantages of the 2.5D approach. A COMSOL model which preceded the experimental work provided important guidance. The simulation showed that with the 2.5D configuration, having a high ionic conductivity electrolyte, on the order of 1 mS cm^{-1} , would enable full capacity to be reached at a current density of 1 mA cm^{-2}, leading to both a high energy density along with a high power density.[13]

Prior to the COMSOL study, the research was done on ionogel electrolytes.[14] These solution-processable materials are pseudo solid-state electrolytes in which a silica matrix

confines a lithium-conducting ionic liquid at the nanoscale. In addition to exhibiting low impedance interfaces with electrode materials such as LFP (lithium iron phosphate), the ionogel electrolytes possess excellent thermal stability (> 300°C), a wide electrochemical window (> 4.0V vs. Li/Li+) and a conductivity up to 2 mS cm^{-1}. This combination of properties is better than what is commonly achieved with LIPON electrolytes. Thus, based on the COMSOL model and the availability of a suitable electrolyte, research was initiated on the 2.5D battery. The LFP array, prepared by microfabrication methods, consisted of 100 μm diameter rods, an aspect ratio of 5:1 and a pitch of 100 μm. The theoretical areal capacity of 1.4 mAh cm^{-2} was achieved at a current density of 50 μA cm^{-2} but increasing the current density to 1 mA cm^{-2} decreases the capacity by only 20% to 1.1 mAh cm^{-2}.

When considering cathode ink development, the overarching objective for this task is to develop a printable cathode ink that can be successfully formed into 3D arrays through the use of DIW. The lead for this task was LLNL since their experience provided excellent insights regarding the ink requirements for 3D printing electrode arrays. Traditional 2D battery electrodes typically use a slurry approach, in which a conductive additive and binder dissolved in a solvent are mixed with the electrochemically active material and doctor bladed to achieve specific mass loadings and electrode thicknesses. However, the slurry requirements for DIW inks are more involved because of the need to deposit high aspect ratio structures and control their spatial alignment along with electrochemical performance. Thus, the ink formulations have rheological and mechanical requirements which traditional slurries do not have. It is expected that the slurry compositions will need to be modified to achieve these properties. From prior work with 2.5D batteries, the first cathode ink material to be developed will be based on $LiFePO_4$ (LFP). Although the tasks for ink development and DIW are separate, we will establish a robust feedback loop between the two activities. One of the best means for determining whether an ink is effective is to carry out a direct writing experiment and to characterize the nature of the written material. Based on these results, which involves examining the physical, mechanical and electrochemical properties of the deposited ink, the team will be able to identify any shortcomings which can then be addressed by altering the ink formulation. The UCLA team will assist the LLNL team by focusing on the electrochemical properties of the ink.

The DIW work will be carried out entirely at LLNL, with intellectual inputs from UCLA. The goal is to produce cathode array structures based on the previously prepared inks. Using the

2.5D simulations developed previously, UCLA will provide the various 3D designs and, specifically, the preferred dimensions of the post, pitch, and needed height. The DIW process will need to establish protocols for varying the dimensions and spatial arrangement of the cathode lattices, as well as the tolerance and variation of array height and diameter. Achieving the finest feature size is limited by the nozzle and the size of the LFP particles in the ink. In order to reach the 20μm level, sub-μm particles must be used which means that nanoscale particles need to be obtained. Another issue to be resolved is adhesion between the lattice layers and the current collector, and the need to make sure that this will be a low resistance contact.

Availability of functional electrode lattices fabricated by DIW will enable us to assemble and test 2.5D batteries. UCLA will lead this effort. The focus of the device assembly will rely on synthesizing the ionogel electrolyte and the ability to infiltrate it into the 3D electrode array structure. Initially, there were concerns that the different LFP composition compared to the one used previously in microfabrication may have different wetting properties, react slightly with the ionogel and cause an impedance at the electrode/electrolyte interface. The team is able to adjust the synthesis of the ionogel accordingly to optimize the performance. Another consideration is the need to incorporate the lithium anode into the battery architecture. The latter will be coordinated with packaging the battery.

One key technological innovation in this project is our use of DIW to print the electrode arrays which are the central design element in the 2.5D battery. 2.5D batteries are also innovative as this design combines the advantages of a 3D battery architecture, namely high energy and power density (area normalized) relative to conventional batteries, with a simpler fabrication process and, potentially, cost advantages. The use of DIW to fabricate this battery architecture offers great design freedom in terms of changing dimensional parameters of the array as well as the prospect of rapid production and, potentially, a large-scale manufacturing process.

In order to realize this technological innovation, our project integrates three objectives which were mentioned previously. The development of a cathode ink enables 3D printing of cathode rods which, when combined with the ionogel electrolyte and Li planar electrode, enables full 2.5D batteries to be fabricated. The energy and power considerations of the 2.5D batteries are largely determined by the dimensional parameters of the cathode array.[13] We have previously prepared LFP arrays by microfabrication methods and have a good data base of relevant properties.

Chapter 3. *Results and Discussion*

3.1.1. *Cathode Ink Development*

The development of cathode inks represents a key step in the DIW process as it enables the array structure to be fabricated. The ink is a dispersion or slurry of various components: the electrochemically active material, conductive additives, and polymer binder. Redox reactions occurring in the active material (in our case, LFP) require electronic conduction to provide rapid charge transfer. However, the low electronic conductivity of LFP requires an additive, such as carbon black, to provide an appropriate level of electronic conduction. A binder, such as polyvinylidene fluoride (PVDF), is also added to ensure that the LFP and carbon particles are suitably bound and in close proximity. In addition to exhibiting excellent electrochemical properties, these inks must also possess the necessary rheology and wetting characteristics for printing, as well as the ability to form arrays of vertical posts with careful dimensional control that is maintained upon drying. Furthermore, the dried posts must have approximately 30% porosity so that the electrolyte can penetrate the rod and provide the necessary ionic conduction. Ideally, this porosity will be interconnected, with sizes generally ranging from 0.1 to 2 μm.

3.1.1.1. Development of baseline ink formulations

Two commercially available LFP powders were obtained from Dakota Lithium (Dakota) and American Elements (AE). The materials were physically characterized to verify the material phase and determine the particle size distributions for the ink development. Both materials were shown by X-ray diffraction to be phase pure $LiFePO_4$ (Figure 1). SEM images of the powders indicated an average particle size for the Dakota LFP of 1-2 μm while that for the American Elements LFP sub 1μm (figure 1). These two commercially available powders served as the foundation for the ink formulations to be used in the additive manufacturing (AM) printing either by both DIW and templating approaches.

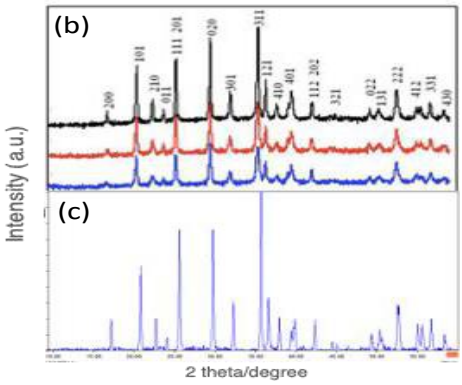

Figure 1. XRD spectra comparing the reference spectra (black, red and blue) to the spectra of the Dakota LFP (bottom spectrum).

Once physically characterized, LFP electrodes were prepared using a tape casting method for fabricating standard planar electrodes. Two different electrode compositions were investigated. One composition was 80% LFP, 10%carbon additives, 10% binder (PVDF) while the second has significantly less LFP (70% LFP, 8% graphite, 13% carbon black and 9% PVDF). This second composition was also used for testing in the initial DIW printing studies. For screening purposes, the electrodes were made at a loading of 2.0 mg cm^{-2}. It should be noted that these initial baseline ink compositions served as the foundation for designing more specific ink formulations for AM processes.

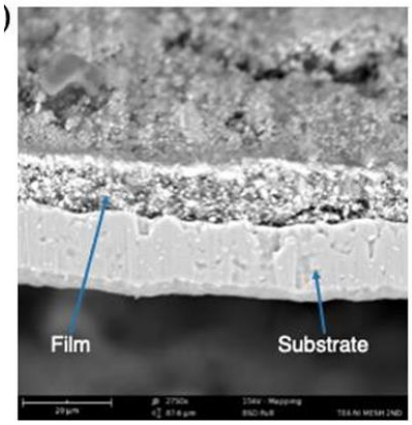

Figure 2. Cross-section of the 2.0 mg cm^{-2} electrode. The electrode is ~40% porous with a film thickness of ~13-15 □m.

The thickness of the 2.0 mg cm^{-2} electrodes was measured using cross sectional SEM of the electrode. The thickness was determined to be ~13-15μm (Figure 2). The porosity of the tape cast electrodes was determined by image analysis to be ~40%. This value exceeded the original target porosity of 25% set for the initial electrode development.

The prepared electrodes were then assembled into a coin cell, in a half-cell arrangement, with lithium metal as the counter electrode and either 1M $LiClO_4$ in propylene carbonate (PC) or 1M $LiClO_4$ in EC:DMC as the electrolyte. This half-cell experimental arrangement enabled us to rapidly determine electrochemical properties of LFP electrodes of various compositions. Table 1 summarizes the electrochemical properties of electrodes prepared with the LFP materials obtained from Dakota and American Elements At a rate of C/10 and even higher, both materials meet or exceed the goal of achieving a lithium capacity within 75% of the theoretical capacity of LFP (taken as 170 mAh g^{-1}). Specific values depend on the electrolyte. Based on these results, all subsequent electrochemical experiments were carried out using 1 M $LiClO_4$ in PC. The galvanostatic curves at C-rates between C/10 and 2C are shown in Figure 3.

Table 1. Summary of electrochemical testing done in the screening of commercial LFP purchased from Dakota and American Elements.

Supplier	Slurry Composition	Electrolyte	Loading (mg cm^{-1})	C/10 (mAh g^{-1})	C/5 (mAh g^{-1})	C/2 (mAh g^{-1})	C (mAh g^{-1})
Dakota	80:10:10	$LiClO_4$ in PC	2.0	130	120	115	110
Dakota	70:8:13:9	$LiClO_4$ in PC	2.0	170	160	155	140
Dakota	70:8:13:9	$LiClO_4$ in EC:DMC	2.0	125	122	117	110
American Elements	80:10:10	$LiClO_4$ in PC	2.0	135	128	120	110
American Elements	70:8:13:9	$LiClO_4$ in EC:DMC	2.0	100	95	85	75

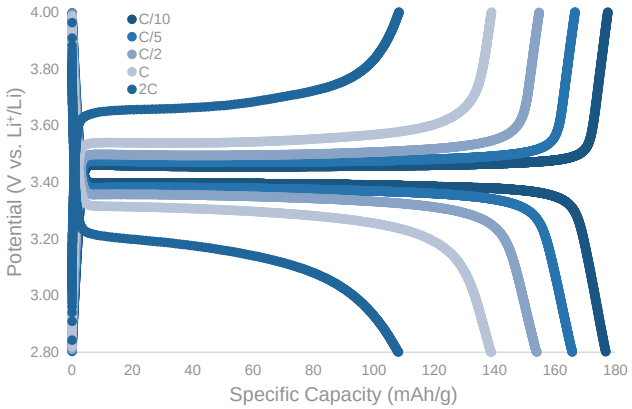

Figure 3. Representative capacity - voltage curve for Dakota LFP with composition 70:8:13:9 (LFP:Graphite:Carbon Black:PVDF).

3.1.1.2. Determining ink compatibility with AM fabrication

The identified baseline ink compositions were then modified to be compatible to the DIW printing process. In collaboration with LLNL, two compositions were identified. The first ink, which will be referred to as LLNL1 was 85% LFP, 7.5% carbon black and 7.5% PVDF. The second ink, referred to as LLNL 2, is 82.5% LFP,8.75% carbon black and 8.75% PVDF. These inks met the appropriate shear-thinning behavior which is required to achieve high-quality DIW printed structures that retain their shape. In addition, we found that changing the carbon content proved to be the most effective parameter in preventing both cracking and delamination of the printed film. Both inks readily met the rheological parameters indicated by LLNL for the LFP-based ink is to have an apparent viscosity and shear yield stress in the range of 10^3 –10^4 Pa·s at 1 s^{-1}, and 10^2 –10^3 Pa, respectively (Figure 4).

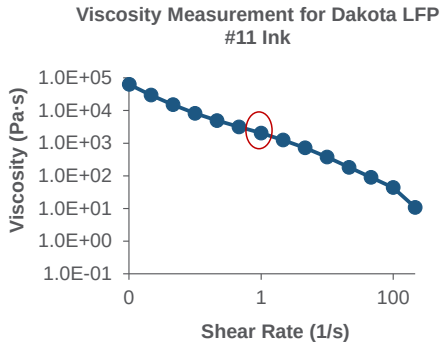

Figure 4. Viscosity measurement of the LFP ink with target viscosity circled in red.

In addition to meeting the rheological goals, initial printing of 2D planar electrodes was demonstrated with both of these ink compositions (Figure 5). The effects of particle size and nozzle diameter were important in achieving uniform printing. SEM of 2D printed electrodes of LLNL1 fabricated via DIW are shown in Figure 6. The samples were approximately 150μm thick with porosities of 47%.

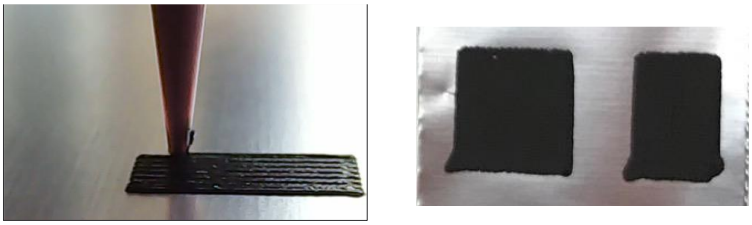

Figure 5. DIW printing of LFP ink (left) and printed electrodes after drying (right). The materials show good adhesion to the substrate with no cracking.

We also carried out galvanostatic measurements to evaluate the electrochemical properties of LLNL 1 and LLNL 2 (Table 2). For these experiments we prepared tape cast electrodes of both compositions and with both commercial LFP powders. The resulting coin cell tests showed that these compositions exhibit very good capacities, well above 75% of theoretical at rates from C/10 to C/2, This is an important result because it shows that we now have an ink which can not only be printed effectively but also possesses appropriate electrochemical behavior.

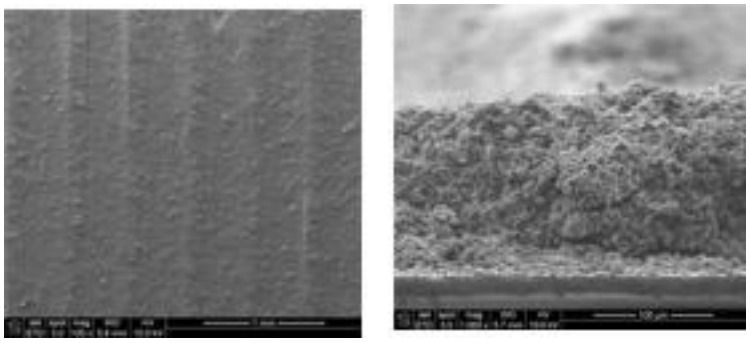

Figure 6. LLNL1 Dakota 2D printed electrode (left) planar view showing the printed rows (scale bar 1mm) and (right) cross- sectional view (scale bar 100□m).

Table 2. Summary of the electrochemical properties of LLNL compositions used in DIW printing.

Supplier	Slurry composition	Electrolyte	Loading mg/cm^2	Method of Measurement	C/10 (mAhg^{-1})	C/5 (mAhg^{-1})	C/2 (mAhg^{-1})
Dakota	85:7.5:7.5 (LLNL1)	$LiClO_4$ in EC:DMC	2.0	2 electrode coin cell	140	135	130
Dakota	82.5:8.75:8.75 (LLNL2)	$LiClO_4$ in EC:DMC	2.0	2 electrode coin cell	146	125	120
American Elements	85:7.5:7.5 (LLNL1)	$LiClO_4$ in EC:DMC	2.0	2 electrode coin cell	155	150	130
American Elements	82.5:8.75:8.75 (LLNL2)	$LiClO_4$ in EC:DMC	2.0	2 electrode coin cell	150	140	130

3.1.1.3. Processing and electrochemical properties of AM fabricated cathodes

We determined that the compositions modified by LLNL for DIW of 2D

electrodes exhibited very good capacities when fabricated in coin cells (Table 2). We also used SEM to characterize the microstructure of the printed electrodes (Figure 6). We now investigated the electrochemical properties of the actual 2D DIW electrodes. It is important to mention that the printed electrodes had a loading of 14 mg cm^{-2}, far greater than the 2.0 mg cm^{-2} loading evaluated previously Because of the larger electrode size, the printed electrodes were tested in flooded 3 electrode cells with lithium as both the counter and reference electrode. The results of these experiments are summarized in Table 3.

Table 3. Summary of electrochemical results for 2D printed electrodes of Dakota and American Elements LLNL 1 and LLNL2.

Supplier	Slurry composition	Electrolyte	Loading (mg cm^{-1})	Method of Measurement	C/10 ($mAhg^{-1}$)	C/5 ($mAhg^{-1}$)	C/2 ($mAhg^{-1}$)
Dakota	85:7.5:7.5 (LLNL1)	$LiClO_4$ in EC:DMC	14.0	3 electrode flooded cell	140	-	-
Dakota	82.5:8.75:8.75 (LLNL2)	$LiClO_4$ in EC:DMC	14.0	3 electrode flooded cell	140	134	120
American Elements	85:7.5:7.5 (LLNL1)	$LiClO_4$ in EC:DMC	14.0	3 electrode flooded cell	120	95	-
American Elements	82.5:8.75:8.75 (LLNL2)	$LiClO_4$ in EC:DMC	14.0	3 electrode flooded cell	110	67	-

At a rate of C/10, both Dakota LLNL1 and LLNL2 electrodes achieved a acapacity of 140 $mAhg^{-1}$ which is 83% of the theoretical capacity for LFP while that of American Elements is more than 65%. These values far exceed the target of 50% of theoretical capacity set and clearly shows that these compositions possess suitable electrochemical properties. The results also show that the capacity of the 2D electrodes with 14.0 mg cm^{-2} loading was comparable to those of the 2.0 mg cm^{-2} samples. The capacitance – voltage curves for Dakota LLNL 2 are shown in Figure 7.

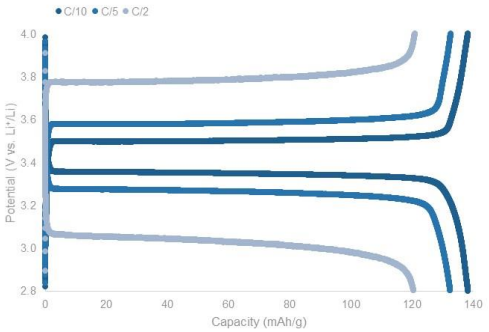

Figure 7. Capacity – Voltage curve for LLNL 2 printed by DIW on a stainless steel current collector.

The electrical conductivities of Dakota LLNL 1 and Dakota LLNL 2 electrodes were measured. The electrodes were fabricated using the same tape casting method as that employed for the electrochemical measurements with a loading of 2.0 mg/cm^2. The reported conductivities (two-lead method) ranged between 0.24 and 0.20 mS cm $^{-1}$ respectively. These values are somewhat more conductive than the target electrical conductivity goal of 0.1mS/cm, and are considered to be beneficial for achieving higher rate properties.

In addition to galvanostatic measurements, we also carried out cyclic voltammetry (CV) on tape cast electrodes using a 2 electrode coin cell format and an electrolyte of 1M $LiClO_4$ in 1:1 volume ratio of EC:DMC. The four different electrode compositions shown in Table 3 were tested. The results for LLNL 1 at sweep rates between 0.1 and 1.0 mVs^{-1} (Figure 8) are consistent with literature as there are prominent redox peaks on both reduction and oxidation and the system is highly reversible

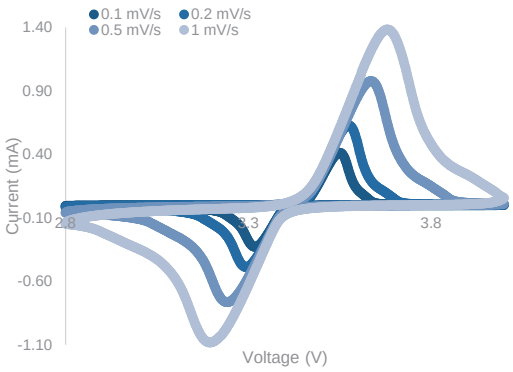

Figure 8. CV of Dakota LLNL1 tape cast electrode at scan rates between 0.1 and 1.0 mVs^{-1}.

3.1.1.4. Optimizing ink formulation for high performance cathodes

Initial baseline electrochemical behavior for the 2D printed electrodes were used to further refine the ink formulations. As shown in Table 3, at a rate of C/10, both Dakota LLNL1 and LLNL2 electrodes achieved a capacity of 140 $mAhg^{-1}$ which is 83% of the theoretical capacity, baseline targets are typically 80% of theoretically capacity. Moreover, this value was achieved with 14.0 mg cm^{-2} loading, a loading consistent with commercial electrodes and substantially greater than the loading used in typical laboratory electrodes (1 to 2 mg cm^{-2}).

We also investigated the cycling of half-cells of the Dakota LLNL1 2D printed electrodes. These experiments were carried out in a flooded 3 neck cell using the same electrolyte as that used in the capacity experiments indicated in Table 3. The capacity and coulombic efficiency over 25 cycles are shown in figure 9.

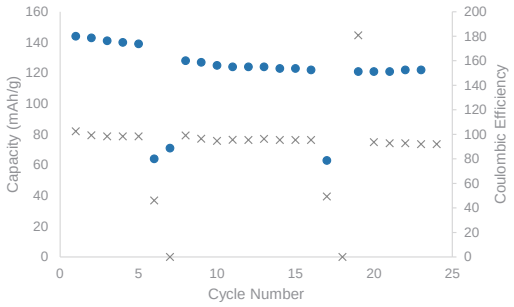

Figure 9. Capacity of the 2D printed Dakota LLNL 1 electrode composition when cycled at C/10. The decreases in capacity and coulombic efficiency are due to power outages during the cycling.

The materials exhibit extremely good reversibility as well as good capacity retention, levelling off to 122 mAh g^{-1} (~72% of theoretical). The fluctuations in electrochemical performance occurred because of a power outage and, thus it is good to see that both capacity and coulombic efficiency returned to pre-outage values when the power was reinstated. Additional experiments are in progress to validate these cycling results.

Electrochemical experiments were also initiated in which an ionic liquid electrolyte substituted for the organic electrolyte. These experiments provide an indication of the compatibility of LFP inks with this electrolyte. Even though the capacity (American Elements LLNL 2) was slightly lower when using an ionic liquid electrolyte of 0.5M LiTFSI in butyl methylimidazolium (BMI) TFSI compared to the organic electrolyte (see Table 4), the difference was < 10% and the capacity was greater

than 80% of theoretical.

Table 4. Summary of electrochemical results showing the difference in capacity when using organic and ionic liquid electrolytes with AE LLNL1 and LLNL2.

Supplier	Slurry composition	Electrolyte	Loading (mg cm^{-1})	Method of Measurement	C/10 ($mAhg^{-1}$)	C/5 ($mAhg^{-1}$)	C/2 ($mAhg^{-1}$)
American Elements	82.5:8.75:8.75 (LLNL2)	0.5M LiTFSI BMITFSI	2.0	2 electrode coin cell	138	106	22
American Elements	85:7.5:7.5 (LLNL1)	0.5M LiTFSI BMITFSI	2.0	2 electrode coin cell	125	64	45
American Elements	85:7.5:7.5 (LLNL1)	$LiClO_4$ in EC:DMC	2.0	2 electrode coin cell	155	150	130
American Elements	82.5:8.75:8.75 (LLNL2)	$LiClO_4$ in EC:DMC	2.0	2 electrode coin cell	150	140	130

As an initial step toward 3D electrode structures, we demonstrated the DIW of two-layer 3D lattices using the American Elements LLNL1 and LLNL2 inks. The lattices printed well and dried without delaminating (figure 10), The dimensions of the lattice are indicated.

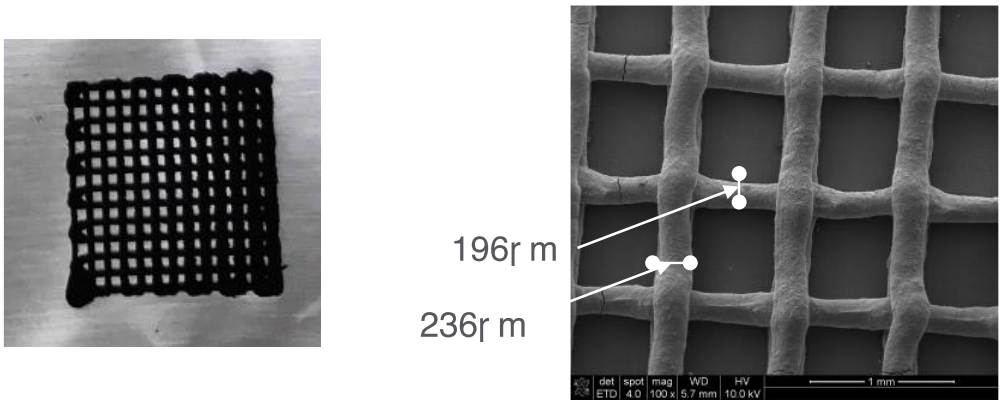

Figure 10. DIW printed 3D electrode based on a lattice geometry. The nominal size of the structure (left) is 1 cm x 1 cm. Careful drying procedures have minimized the presence of cracks on individual ribbons.

Development of LFP inks which enable the fabrication of 2D electrodes by additive manufacturing processes were verified using several metrics. Electrochemically, the inks demonstrated 80% of the theoretical capacity (170 mAh/g) with at least 25 reversible cycles at a C/10 rate. In general, we have developed two LFP ink formulations which successfully print 2D electrodes by DIW. The resulting electrodes, specifically those using the Dakota LFP material, demonstrated lithium capacities in excess of 80% of the theoretical lithium capacity values of LFP (Table 3). The American Elements LFP offers slightly less capacity (70%). We have also cycled half-cells of the 2D printed electrodes for 25 cycles at the C/10 rate. The electrode displays

excellent reversibility with very good capacity retention (72% of the theoretical value), a decrease of only 10% from the initial capacity value. The initial screening and development process for the inks have given a basis for moving on to print the 3D structures.

3.1.2. *3D Printing of Electrode Structures*

3.1.2.1. Development of variable array configurations based on LFP inks

The goal of this task was demonstrate printing of electrodes with varying dimensions. Originally, the intent was to print pillar electrodes, however, because of the versatility of the DIW process, we were able to print a far more robust geometry based on a lattice-like configuration. Initially, printed lattices were demonstrated and printed using 3 and 5 layers with open areas of approximately 40% using both the Dakota LFP and the American Elements LFP. SEM was used to verify the consistency of these printed lattices and there was little variability of printing between the layers. Inks were slightly modified from this initial iteration because of lattice cracking seen during drying. The same geometries were printed with a slightly modified ink and showed little cracking. Based on the drying results, the geometry of the printed lattices were then optimized. All lattices with optimized geometry were printed using the American Elements LFP LLNL2 recipe. This decision was made after evaluating the electrochemical properties of the inks as a printed lattice.

(a)

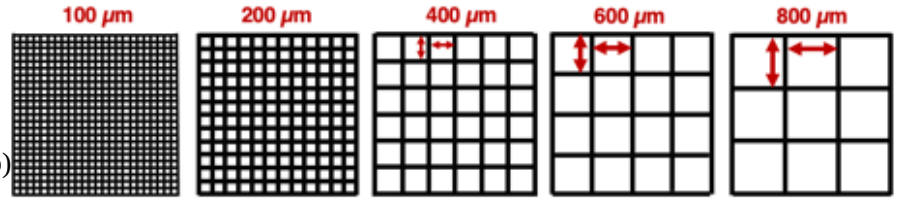

(b)

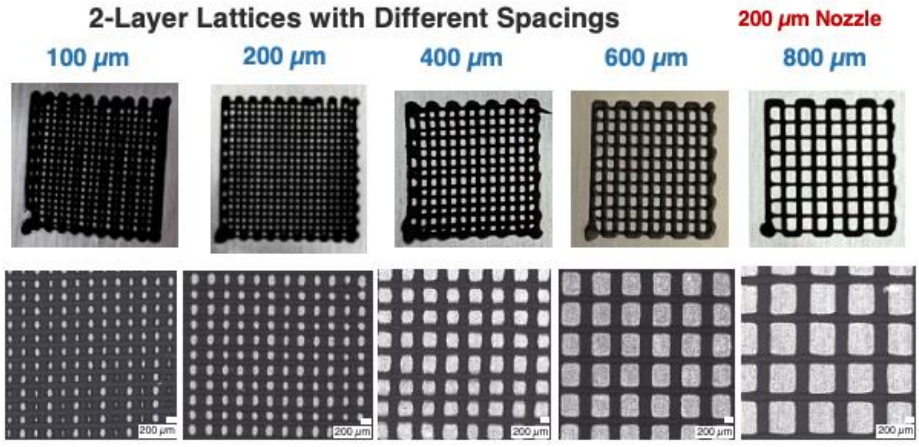

Figure 11. (a) Lattice designs and (b) optical images for 3D printed lattices with varying pitch lengths from 100μm to 800μm spacing.

For the optimized printed lattices, the line dimension for the pitch varies from 100μm to 800μm, leading to areal solid fractions between 54% and 16%, which corresponds to open areas of 46% and 84% respectively. Lattices with pitch spacings from 100μm to 800μm were successfully printed using a 200μm nozzle and AE LLNL2 ink. Optical microscope images showed that during printing the shape of the lattices remained consistent and there was not a large amount of bleeding of the ink during the printing or drying processes (Figure 11). There was some delamination of the electrodes, mostly seen in the 100, 200, and 400μm lattices. While the lattices did delaminate, the lattice structures remained intact and did not fracture or spall. These delaminated lattices facilitated electrochemical testing in coin cells. The lattice designs and optical microscope images of the printed 2 layer lattices can be seen in figure 11.

Work was also done on using the templating method to create uniform pillar electrodes. The process used a printed pillar template that would be immersed in PDMS and cured. The template was made from PDMS to ensure its flexibility, and allow for the template to be peeled away once filled with the LFP ink. The improved templating process and experimental results are shown in figure 12.

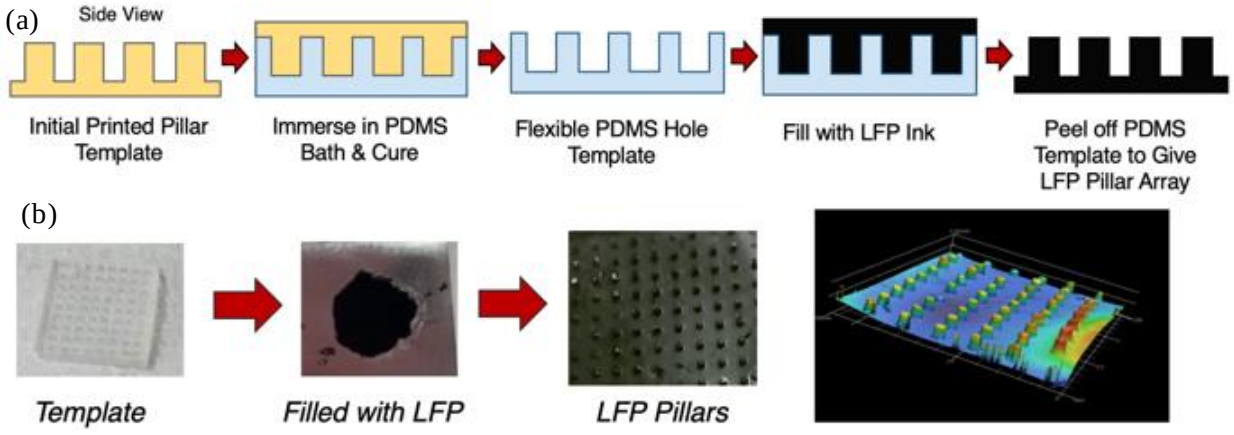

Figure 12. (a) Proposed process flow of the template fabrication for LFP pillar electrodes. (b) Experimental images of the templating process and resulting pillar array.

3.1.2.2. Electrochemical properties of 3D electrode arrays

Utilizing the printed lattices of various dimensions, testing was done to determine their electrochemical properties and optimize the geometry for the printed electrodes. In addition to understanding the electrochemical properties, another important metric was to achieve 1mAh/cm^2 for the areal capacity of the DIW printed lattice configuration. Galvanostatic and potentiostatic testing was done on the electrodes of varying geometries to determine their electrochemical properties. The relationship among lattice spacing, areal solid fraction, predicted areal capacity and experimental areal capacity was determined (table 5). The calculation for the areal solid fraction and predicted areal capacity assumes the same line diameter for each of the lattices, with an ink density calculated from previous lattices. The areal capacity is then based on the theoretical capacity for LFP and the expected loading.

Table 5. Predicted Areal Capacity based on modified lattice spacing.

Number of Layers	Size of Printing Nozzle (μm)	Lattice Spacing (μm)	Areal Solid Fraction	Predicted Areal Capacity (mAh/cm^2)	Experimental Areal Capacity (mAh/cm^2)
2	200	100	54%	1.13	1.12
2	200	200	40%	0.84	0.71
2	200	400	26%	0.56	0.55
2	200	600	20%	0.42	0.46
2	200	800	16%	0.34	0.51
3	200	200	39%	1.27	2.38
2	250	200	44%	1.17	1.17
2	250	400	30%	0.81	1.67
2	250	600	23%	0.62	1.46
2	250	800	19%	0.50	1.18

The predicted areal capacities for the 2 layer printed lattices were very close to the experimentally determined values and a 2-layer lattice printed with a 200μm and 100μm spacing, achieved an areal capacity of 1.11mAh/cm^2 which satisfies the milestone requirement (figure 13). All lattices were also tested at varying rates to determine the effect of the lattice geometry on their rate performances (figure 13). Additional means of increasing areal capacity were also explored such as printing with a larger nozzle or increasing the number of lattice layers to increase active material loading. Both increasing the line thickness and number of layers helped to increase the reported energy density, with a 3 layer lattice that was printed using 200μm spacing had an areal capacity of 2.38mAh/cm^2 (table 5). When evaluating the rate capabilities of

the larger nozzle and added layers, it was found that the samples with more layers had better kinetics than those printed with larger nozzles. This feature will be taken into consideration when considering higher areal capacity in future generations of materials and electrodes.

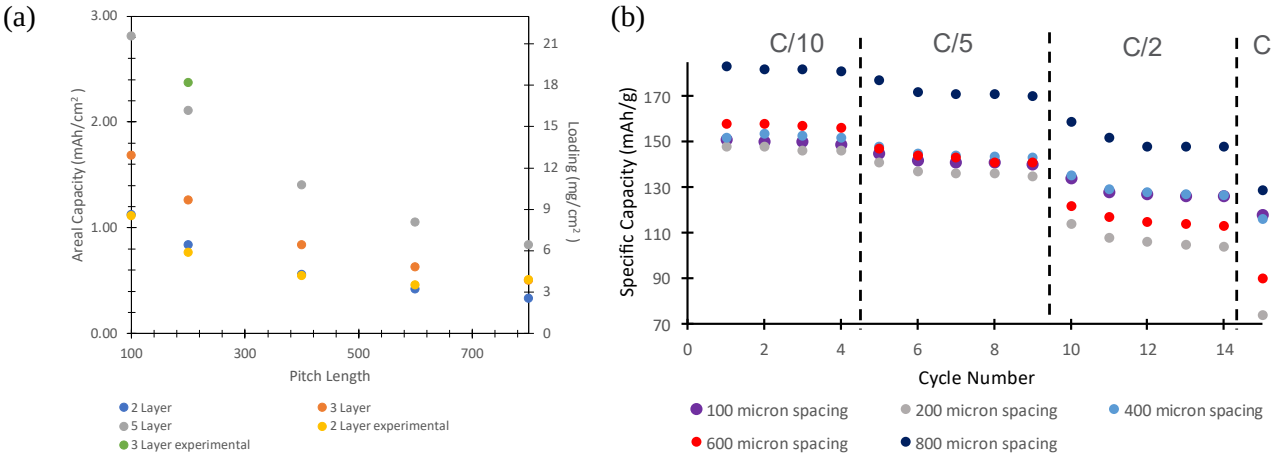

Figure 13. (a) Predicted areal capacity of 3D lattice electrodes with varying pitch length for 2,3 and 5 layer lattices. Experimental results at C/10 are shown for the 2-layer and 3-layer electrodes. (b) Specific capacity of 3D printed lattices with various pitch dimensions as a function of C-rate in a flooded 3-neck with organic electrolyte.

3.1.3. *2.5D Battery Fabrication and Testing*

3.1.3.1. Development of components for 2.5D battery

An important consideration for optimizing battery performance is the wetting behavior and interfacial resistance of the LFP electrode and ionogel electrolyte. Contact angle measurements were taken using tape cast electrodes and ionic liquid electrolyte. The angle was determined to be <6° which is indicative of good surface wetting. Initial testing with incorporating the ionogel showed a low rate capability and a higher than expected interfacial resistance. The high interfacial resistance indicated that there was potentially a surface reaction at the electrode/electrolyte interface, and that the ionic liquid electrolyte might not be penetrating the pores of the electrode even though wetting of the electrode is observed.

Alternative ionic liquid electrolytes and syntheses were explored in order to optimize the system. Both the cation of the ionic liquid and the lithium salt were modified. Following optimization of the ILE, synthesis of the gel was altered in order to improve the overall connectivity of the gel. The parameters investigated included the pH of the ionogel electrolyte and precursors. The ionogel compositions with the highest conductivities were synthesized onto the LFP lattices by drop casting. Using Gravimetric Intermittent Titration Technique (GITT),

measurements were carried out to determine the interfacial resistance via the iR drop. Using an organically modified ionogel, the conductivity and interface resistance was calculated to be 2.11mS cm^{-1} and 120 Ohm cm^2 (figure14).

(a) 200 µm nozzle, 400 µm spacing

*pH	Conductivity ($mS*cm^{-1}$)	Working Electrode Interface ($Ohm*cm^2$)
3-4	0.207	440
4	1.11	390
4-5	3.44	350

(b) 200 µm nozzle, 100 µm spacing

MTMOS:TMOS	Conductivity ($mS*cm^{-1}$)	Working Electrode Interface ($Ohm*cm^2$)
1:3	2.11	120
0:1	1.82	130

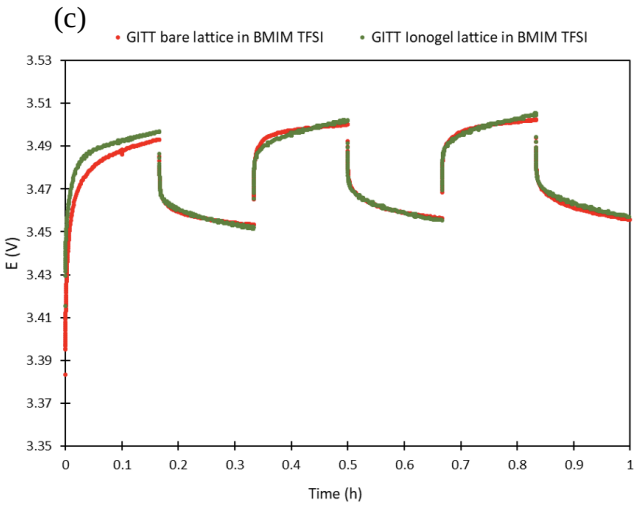

Figure 14. Calculated conductivity and working electrode interface resistance for ionogels of varying (a) pH and (b) methyl content. (c) Gravimetric Intermitted Titration Technique (GITT) measurements for a sample of MTMOS:TMOS content 1:3.

Additional means of optimizing the ionogel involved reducing salt content and solvent exchanging the ILE for an organic electrolyte (figure 15). The organic electrolyte demonstrates better kinetics than the ionic liquid electrolyte while helping maintain the lower interfacial resistance.

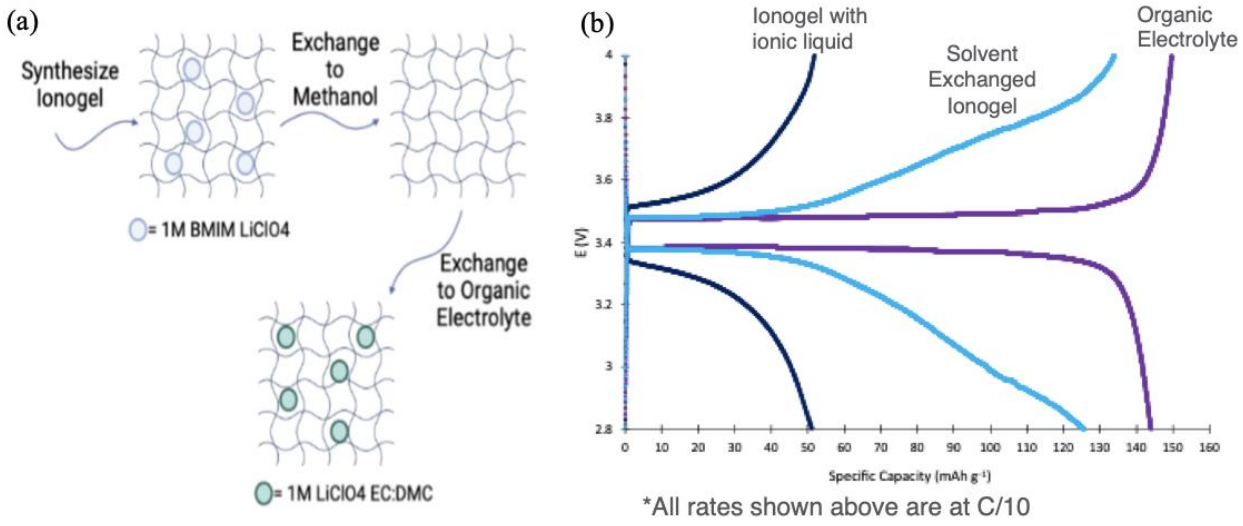

Figure 15. (a) Outlines the ionogel solvent exchange process to remove the ILE from the silica matrix and exchange in organic electrolyte. (b) Galvanostatic charge/discharge curves comparing an LFP electrode

with an ionogel with ionic liquid, a solvent exchanged ionogel, and in organic electrolyte at a rate of C/10.

3.1.3.2. Assembly and testing of 2.5D batteries

The goal for initial integration of the 3D cathode/ionogel into the full device was to establish an areal capacity of 1.4mAh/cm^2, and charging rates of at least 5C. The pre-cycling method described in the section prior was expanded upon and it was found that treatments at a rate of C/10 in a flooded cell helped to ensure that a complete electrolyte exchange occurred and that the ionogel was thoroughly infiltrated with electrolyte. The resulting kinetics were an improvement when compared to using an intermediate solvent.

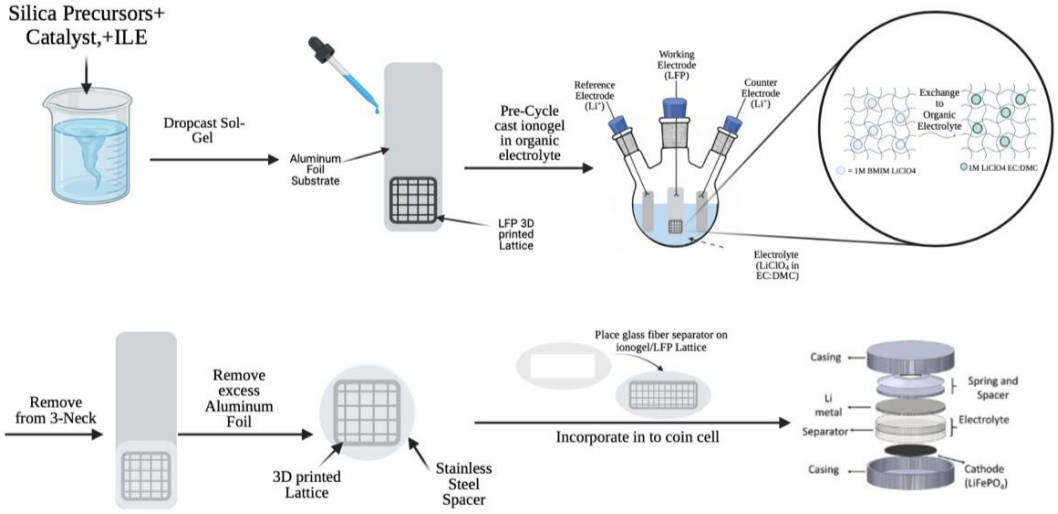

Figure 16. Optimized fabrication process flow for full 2.5D battery.

Upon assembling the full 2.5D device, there was an initial contact problem between the ionogel and the lithium metal anode due to uneven coating of the gel. To help mitigate this issue, a glass fiber separator with a window cutout for the lattice was used in device fabrication. The addition of the separator helped with the contact issue and a full 2.5D battery was fabricated. An optimized process was developed for assembling the 2.5D device that can be seen in figure 16. Alongside the process for assembling devices, additional substrates were used to help improve overall performance. In the optimized system, a metric of 2.4mAh/cm^2 areal capacity was established for the full device. This performance metric will enable us to reach the DOE goals when scaling the device.

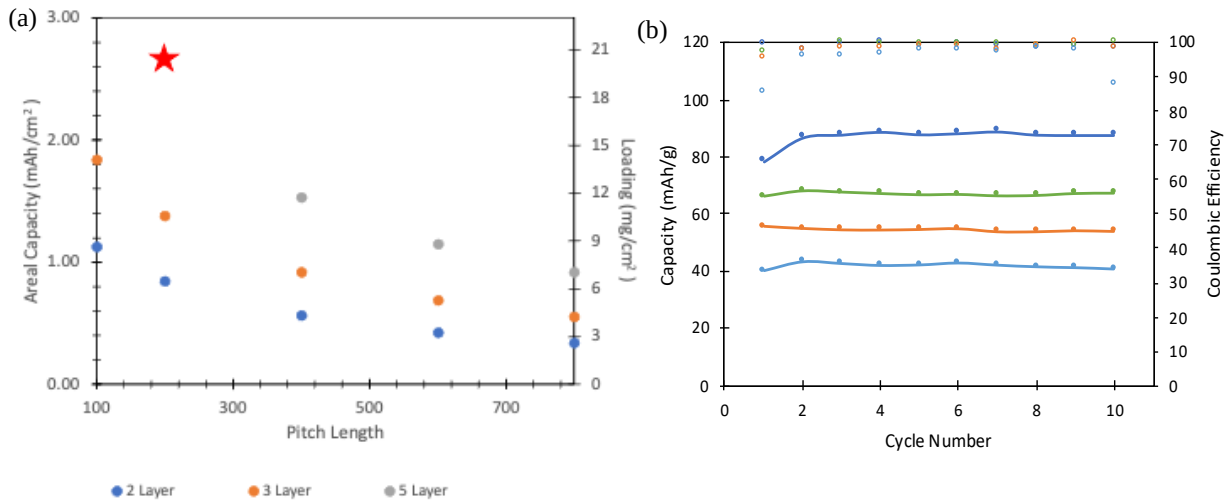

Figure 17. (a) Predicted areal capacity of 2, 3 and 5 layer lattices with varying pitch length. The red star is the experimental areal capacity of a 5 layer lattice. (b) Specific capacity and coulombic efficiency of device with a 5 layer lattice.

Electrodes based on using five layer lattices were integrated into a 2.5D battery. The tested devices had an experimental areal capacity of 2.75mAh/cm^2 (figure 17). Rate testing was also done on this device, and rates from C/10 up to 5C. At a rate of C/10 147mAh/g (87% theoretical lithium capacity) was achieved, and coulombic efficiency was 98-100%. The coulombic efficiency at rates C/2 to 5C are reported in figure 17 above. Operating the device at a rate of 5C and achieving an areal capacity of 2.75mAh/g surpasses the original areal capacity goal.

Chapter 4. *Benefits Assessment*

The low capital equipment cost of DIW printers (<$10K each) is relatively well documented in the literature. Although DIW for volume battery manufacturing is still in the R&D phase (as proposed in this project), some earlier work from LLNL (https://str.llnl.gov/january-2015/marrgraff) has demonstrated the potential of large area DIW-production. In that work, LLNL demonstrated that silicone cushions that are 85% cheaper than foams manufactured with legacy approaches can be made in a tenth of the time. Such volume production of cushions has been integrated into weapon systems for national security applications. In addition, we believe DIW has advantages during the initial prototyping of electrode structures due to the design freedom offered by additive manufacturing.

Chapter 5. *Commercialization*

Most of the advances in 3D battery technology have occurred in areas related to consumer electronics as this platform was developed initially for microbattery applications because of its small footprint area. Among the start-up companies who base their designs on 3D configurations and have been in existence for several years are Millibatt (wearables, IOT sensors)[28], Enovix (smartphones, laptops)[29], ADDIONICS (3D electrodes)[30] and Prieto Battery (power tools, EV batteries)[31]. The experience with Prieto Battery is particularly insightful as it shows that scalability issues have limited the development of 3D battery technology in large format applications. The ability to scale the Prieto battery design (based on the 'sponge configuration' presented in 2004)[26,27] has enabled the company to partner with Hercules Electric Vehicles.[32] These examples suggest that the use of DIW as a route for the scalable production of 3D batteries is viable.

The DOE targets for fast charging batteries are 200Wh/kg at 4C but these are for batteries with liquid electrolytes. In contrast, the battery being proposed here is based on an ionogel electrolyte and thus offers a much safer, solid-state design. At the end of the project, the goal is to have a footprint area of 100 cm^2. The specific capacity for the full cell is 130 mAh/g (based on the weights of the electrodes) and this corresponds to an energy density of 210Wh/kg, consistent with the DOE metric. At this time, we have only general cost estimates because the technology is currently at TRL 2 and more needs to be known about the manufacturing parameters. The first task is to scale up the size of the printed electrodes to 10 x 10 cm. This may require changing the order of the fabrication steps or making small alterations to the fabrication procedure. For example, we can start with the 3D DIW-printed LFP lattice, coat it with the ionogel rather than the reverse operation of coating the anode. We will optimize the fabrication process to be most efficient for producing 3D printed electrodes at this larger scale and then explore commercialization options at that time.

Chapter 6. *Accomplishments*

All of the project objectives under this award were successfully completed and we were able to show the development of a 2.5D battery. Manufacturing tasks have been identified and a program directed at achieving a large format full 3D battery is underway through a new EERE award. Additional Accomplishments include:

- 2022 Vehicles Technologies Annual Merit Review, Poster Presentation (June 21-23, 2022).
- ACS Fall Meeting Sustainability in a Changing World, Invited Keynote (August 21-25, 2022).
- Development of 3D LFP Lattices and Understanding of Their Transport Properties, *In Preparation.*
- Transport Properties in Amorphous Silica and Amorphous Metal Oxide Materials. P.E. McNeil, *Thesis in Preparation* (2023).
- Design and Manufacturing of Non-Planar and Solid State Lithium Ion Batteries. M.T. Fox, *Thesis in Preparation* (2023).

Chapter 7. *Conclusions*

In evaluating designs for improving both the areal capacity and rate capability of the 2.5D battery, it was established that higher loadings and optimized geometries in both the planar and z direction were needed to achieve the desired performance. This was accomplished by increasing the number of layers in lattices with an optimized geometry, using a 200μm nozzle to achieve 200μm spacing, and printing up to 5 layers total. The increased number of lattice layers brought the loading to approximately 20 mg/cm^2. The resulting experimental areal capacity of the sample with high loading was 2.75mAh/cm^2, above the initial goal of 2.4mAh/cm^2. In addition, the device was cycled at rates up to 5C, while still demonstrating a coulombic efficiency of 98-100%. The performance of these devices establishes that using DIW in the fabrication of 3D battery designs with solid state architectures offers a promising direction for battery technology.

Chapter 8. *Recommendations*

In order to achieve the metrics outlined by the DOE, it would be beneficial for the commercialization of this device to expand from the 2.5D device to a 3D device. As indicated in the chapter on commercialization, improved performance metrics can be achieved by using the z-direction to increase electrode loading. By using a compatible anode material of appropriate loading, the total energy of the battery can be increased further. During the next EERE project funding period, we will be investigating this approach along with the goal of fabricating larger format batteries by DIW. Demonstrating the ability to rapidly and effectively print the anode and cathode material as well as increase electrode size will enable us to evaluate the potential of utilizing DIW to support large scale battery manufacturing at a cheaper cost than current manufacturing methods. Continued improvements in the ionogel material will also be needed to ensure the compatibility of the electrolyte with an anode material as well as the cathode.

References

1. Hart, R. W.; White, H. S.; Dunn, B.; Rolison, D. R., 3-D Microbatteries. Electrochemistry Communications 2003, 5 (2), 120-123.
2. Long, J. W.; Dunn, B.; Rolison, D. R.; White, H. S., Three-Dimensional Battery Architectures. Chemical Reviews 2004, 104 (10), 4463-4492.
3. Baggetto, L.; Niessen, R. A. H.; Roozeboom, F.; Notten, P. H. L., High Energy Density All-Solid-State Batteries: A Challenging Concept Towards 3D Integration. Advanced Functional Materials 2008, 18 (7), 10571066.
4. Dokko, K.; Sugaya, J.-i.; Nakano, H.; Yasukawa, T.; Matsue, T.; Kanamura, K., Sol–gel fabrication of lithium-ion microarray battery. Electrochemistry Communications 2007, 9 (5), 857-862.
5. Chandrasekaran, S.; Yao, B.; Liu, T. Y.; Xiao, W.; Song, Y.; Qian, F.; Zhu, C.; Duoss, E. B.; Spadaccini, C. M.; Li, Y.; Worsley, M. A., Direct ink writing of organic and carbon aerogels. Materials Horizons 2018, 5 (6), 1166-1175.
6. Zhu, C.; Liu, T. Y.; Qian, F.; Han, T. Y. J.; Duoss, E. B.; Kuntz, J. D.; Spadaccini, C. M.; Worsley, M. A.; Li, Y., Supercapacitors Based on Three-Dimensional Hierarchical Graphene Aerogels with Periodic Macropores. Nano Letters 2016, 16 (6), 3448-3456.
7. Qi, Z.; Ye, J. C.; Chen, W.; Biener, J.; Duoss, E. B.; Spadaccini, C. M.; Worsley, M. A.; Zhu, C., 3DPrinted, Superelastic Polypyrrole-Graphene Electrodes with Ultrahigh Areal Capacitance for Electrochemical Energy Storage. Adv Mater Technol-Us 2018, 3 (7).
8. Min, H.-S.; Park, B. Y.; Taherabadi, L.; Wang, C.; Yeh, Y.; Zaouk, R.; Madou, M. J.; Dunn, B., Fabrication and properties of a carbon/polypyrrole three-dimensional microbattery. Journal of Power Sources 2008, 178 (2), 795-800.
9. Hur, J. I.; Smith, L. C.; Dunn, B., High Areal Energy Density 3D Lithium-Ion Microbatteries. Joule 2018, 2 (6), 1187-1201.
10. Cirigliano, N.; Sun, G.; Membreno, D.; Malati, P.; Kim, C. J.; Dunn, B., 3D Architectured Anodes for Lithium-Ion Microbatteries with Large Areal Capacity. Energy Technology 2014, 2 (4), 362-369.
11. Ashby, D. Ionogels: Addressing the Challenges of Lithium Ion Solid Electrolytes. University of California, Los Angeles, Los Angeles, CA, 2018.
12. Talin, A. A.; Ruzmetov, D.; Kolmakov, A.; McKelvey, K.; Ware, N.; El Gabaly, F.; Dunn, B.; White, H. S., Fabrication, Testing, and Simulation of All-Solid-State Three-Dimensional Li-Ion Batteries. ACS Applied Materials & Interfaces 2016, 8 (47), 32385-32391.
13. McKelvey, K.; Talin, A. A.; Dunn, B.; White, H. S., Microscale 2.5D Batteries. Journal of The Electrochemical Society 2017, 164 (12), A2500-A2503.
14. Ashby, D. S.; DeBlock, R. H.; Lai, C.-H.; Choi, C. S.; Dunn, B. S., Patternable, Solution-Processed Ionogels for Thin-Film Lithium-Ion Electrolytes. Joule 2017, 1 (2), 344-358.
15. Zheng, X. Y.; Smith, W.; Jackson, J.; Moran, B.; Cui, H. C.; Chen, D.; Ye, J. C.; Fang, N.; Rodriguez, N.; Weisgraber, T.; Spadaccini, C. M., Multiscale metallic metamaterials. Nature Materials 2016, 15 (10), 1100-+.
16. Zheng, X. Y.; Lee, H.; Weisgraber, T. H.; Shusteff, M.; DeOtte, J.; Duoss, E. B.; Kuntz, J. D.; Biener, M. M.; Ge, Q.; Jackson, J. A.; Kucheyev, S. O.; Fang, N. X.; Spadaccini, C. M., Ultralight, Ultrastiff Mechanical Metamaterials. Science 2014, 344 (6190), 1373-1377.
17. Zhu, C.; Han, T. Y. J.; Duoss, E. B.; Golobic, A. M.; Kuntz, J. D.; Spadaccini, C. M.; Worsley, M. A., Highly compressible 3D periodic graphene aerogel microlattices. Nature Communications 2015, 6.
18. Yao, B.; Chandrasekaran, S.; Zhang, J.; Xiao, W.; Qian, F.; Zhu, C.; Duoss, E. B.; Spadaccini, C. M.; Worsley, M. A.; Li, Y., Efficient 3D Printed Pseudocapacitive Electrodes with Ultrahigh MnO2 Loading. Joule 2019, 3 (2), 459-470.

19. Shusteff, M.; Browar, A. E. M.; Kelly, B. E.; Henriksson, J.; Weisgraber, T. H.; Panas, R. M.; Fang, N. X.; Spadaccini, C. M., One-step volumetric additive manufacturing of complex polymer structures. Sci Adv 2017, 3 (12).
20. Hensleigh, R. M.; Cui, H.; Oakdale, J. S.; Ye, J. C.; Campbell, P. G.; Duoss, E. B.; Spadaccini, C. M.; Zheng, X.; Worsley, M. A., Additive manufacturing of complex micro-architected graphene aerogels. Materials Horizons 2018, 5 (6), 1035-1041.
21. Tian, X.; Jin, J.; Yuan, S.; Chua, C. K.; Tor, S. B.; Zhou, K., Emerging 3D-Printed Electrochemical Energy Storage Devices: A Critical Review. Advanced Energy Materials 2017, 7 (17), 1700127.
22. Fu, K.; Yao, Y.; Dai, J.; Hu, L., Progress in 3D Printing of Carbon Materials for Energy-Related Applications. Advanced Materials 2017, 29 (9), 1603486.
23. Kim, I.; Park, J.; Nam, T.-H.; Kim, K.-W.; Ahn, J.-H.; Park, D.-S.; Ahn, C.; Wang, G.; Ahn, H.-J., Electrochemical properties of an as-deposited LiFePO4 thin film electrode prepared by aerosol deposition. Journal of Power Sources 2013, 244, 646-651.
24. Delannoy, P. E.; Riou, B.; Brousse, T.; Le Bideau, J.; Guyomard, D.; Lestriez, B., Ink-jet printed porous composite LiFePO 4 electrode from aqueous suspension for microbatteries. Journal of Power Sources 2015, 287, 261-268.
25. Ho, C. C.; Murata, K.; Steingart, D. A.; Evans, J. W.; Wright, P. K., A super ink jet printed zinc–silver 3D microbattery. Journal of Micromechanics and Microengineering 2009, 19 (9), 094013.
26. Sun, K.; Wei, T.-S.; Ahn, B. Y.; Seo, J. Y.; Dillon, S. J.; Lewis, J. A., 3D Printing of Interdigitated LiIon Microbattery Architectures. Advanced Materials 2013, 25 (33), 4539-4543.
27. Izumi, A.; Sanada, M.; Furuichi, K.; Teraki, K.; Matsuda, T.; Hiramatsu, K.; Munakata, H.; Kanamura, K., Development of high capacity lithium-ion battery applying three-dimensionally patterned electrode. Electrochimica Acta 2012, 79, 218-222.
28. www.millibatt.com
29. www.enovix.com
30. www.addionics.com
31. www.prietobattery.com
32. www.prietobattery.com/news-room/